SIAM J. APPL. MATH
Vol. 53, No. 2, pp. 319–339, April 1993

REACTIVE FLOWS IN LAYERED POROUS MEDIA II. THE SHAPE STABILITY OF THE REACTION INTERFACE*

J. XIN†, A. PEIRCE‡, J. CHADAM‡, AND P. ORTOLEVA§

Abstract. The shape stability of the reaction interface for reactive flow in a layered porous medium is studied. This is done using a complete linearized stability analysis in the setting of a free boundary model of this phenomenon. The spectrum of the linearized problem is obtained in the general case, and it is compared with that obtained for homogeneous media in two typical cases.

Key words. modelling geological dissolution fronts, layered porous media, travelling waves, moving free boundary problems, reaction-infiltration instability, asymptotic analysis, homogenization, bifurcation and stability

AMS(MOS) subject classifications. 35R35, 35B32, 86A60, 73H

1. Introduction. In previous work [1]–[3], we studied the problem of reactive flow in a homogeneous porous medium and showed that shape instabilities of the reaction zone occurred only if the reaction caused a porosity change (called the reaction-infiltration instability [1]). The crucial destabilizing feedback mechanism works as follows. If a *porosity/permeability* change occurs, then, through Darcy's law

$$\underline{v} = -\kappa(\varphi)\nabla p \tag{1.1}$$

(where $\kappa(\varphi)$ is a phenomenological function for the permeability as a function of the porosity φ, p is the pressure, and the viscosity is taken to be constant), there can be an alteration of the flow pattern. Note that, if a protrusion (in the porosity level curves) in the reaction zone exists at some time, the flow of the most reactive fluid tends to be focused to the tip of the protrusion via Darcy's law since "inside" the protrusion (the upstream side) the permeability is greater than in the neighboring regions (see Fig. 1.1.). Since additional reactive fluid now arrives at the tip, it tends to advance more rapidly, causing fingering. On the other hand, diffusion from the sides of the protrusion causes the fluid focusing at the tip to be less reactive and hence to decelerate its advancement. The competition between these two mechanisms results in shape

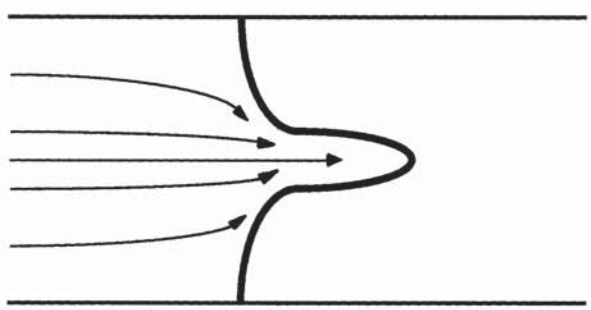

FIG. 1.1. *Focusing of flow to the tip of a porosity level curve.*

* Received by the editors July 8, 1991; accepted for publication (in revised form) February 10, 1992.

† Mathematical Sciences Research Institute, Berkeley, California, 94720. This author was supported by National Science Foundation grant DMS-8505550 held at the Mathematical Sciences Research Institute.

‡ Department of Mathematics and Statistics, McMaster University, Hamilton, Ontario, Canada L8S 4Kl. These authors were supported by the Natural Sciences and Engineering Research Council of Canada.

§ Departments of Chemistry and Geology, Indiana University, Bloomington, Indiana, 47405.

selection (self-organization) of the reaction zone, leading either to the decay of the protrusion, restabilization to a morphologically more complicated advancing reaction zone (fingering), or the temporal development of successively more complicated patterns (tip splitting, budding, and so forth). Understanding this shape selection process has important applications to many geochemical situations (e.g., the diagenesis and evolution of mineral deposits, oil and gas reservoirs, the dynamics of breakout from chemical and nuclear waste repositories, in situ coal gasification, enhanced oil recovery, leaching of minerals, location of roll-front deposits, and so forth [4], [5]).

In this paper, we consider the flow of reactive fluids through layered porous media and determine the effects of the layering on our previous shape stability analysis [1], [2]. This generalization is very important from the viewpoint of applications because much of the world's natural gas can be found in large underground chambers whose sides were naturally formed in a layered pattern. Breakout (puncturing the walls) from these chambers thus requires carrying out the above analysis in the layered region of the walls. Under-pressurized versions of the chambers also occur naturally. Their use as chemical and nuclear waste repositories is quite interesting. A clear understanding of the flow of these highly reactive fluids through the layered walls is crucial to determining the feasibility of this method of storing waste. Mathematically, this has led to a novel asymptotic analysis; coupling homogenization methods with free boundary problems [6].

In § 2 we summarize our mathematical models of the above phenomena. We begin with a system of partial differential equations, which, in a certain physical limit, reduce to an amenable free boundary problem in terms of the macroscopic (averaged) variables for a thin reaction interface. The details of this matched asymptotic analysis are presented elsewhere [6], but a summary is contained here in the Appendix. Section 3 is devoted to the shape stability analysis of this reaction interface. The general criterion is obtained in § 3.2, and a comparison with the homogeneous case is made for two illustrative examples in § 3.3. A detailed summary of these results is provided in § 4 using the concepts and essential parameters developed in this work.

2. Mathematical models. In this section, we present, without details, two mathematical models of the reaction-infiltration process in layered porous media. The first is a coupled set of partial differential equations, which for numerical purposes is quite useful [1], [7], but, from an analytic point of view, is untractable. Taking a physically relevant limit, these equations reduce to a moving free boundary problem for the reaction interface.

2.1. The general partial differential equation model. The complete details of this model can be found in [1] and are presented in complete generality without any hypotheses on the porous medium. The domain of the model is assumed to be an infinite strip: $(x, y) \in (-\infty, \infty) \times [O, L]$. Throughout this region, the rate of increase in porosity $\varphi(x, y, t)$ (equivalently, the rate of dissolution of the soluble minerals) is proportional to the reaction rate

$$\varphi_t = -k(\varphi_f - \varphi)^{2/3}(c - c_{\text{eq}}), \tag{2.1}$$

where k is the reaction rate constant, $\varphi_f(x, y, t)$ is the final porosity after complete dissolution, and $c(x, y, t)$ is the concentration of solute in water with its equilibrium concentration being c_{eq}. The 2/3-power indicates that we are considering surface reactions, but, as we see in the next section, the actual form of the reaction rate in (2.1) does not affect our results since these details are confined to an infinitesimally thin reaction zone when we take the distinguished limit in the next section. The solute concentration per rock volume φc satisfies a mass conservation equation

$$(\varphi c)_t = \nabla \cdot [\varphi D(\varphi) \nabla c + \varphi c \kappa(\varphi) \nabla p] + \rho \varphi_t, \tag{2.2}$$

where D and κ are the porosity dependent diffusion coefficient and permeability, and ρ is the density of the minerals being dissolved. In (2.2), p is the pressure, and Darcy's law, for the velocity $\underline{v}$ in the form (1.1), has been used. Finally, the conservation of water implies that

$$\varphi_t + \nabla \cdot (\varphi \kappa(\varphi) \nabla p) = 0. \tag{2.3}$$

The three equations (2.1)–(2.3) are to be solved for the three unknowns φ, c, p, subject to the imposed asymptotic conditions,

$$c \to 0, \quad \varphi \to \varphi_f, \quad \text{and} \quad p_x \to p'_f \quad \text{as } x \to -\infty \tag{2.4a}$$

and

$$c \to c_{\text{eq}}, \quad \varphi \to \varphi_0, \quad \text{and} \quad p_x \to ? \quad \text{as } x \to +\infty, \tag{2.4b}$$

along with initial data. Conditions (2.4a) say that, at the inlet ($x = -\infty$), the water is free of solute, the porous medium has reached its final altered state in which all the soluble minerals have been previously dissolved out, and a horizontal pressure gradient (equivalently, velocity, through Darcy's law) has been imposed. Similarly, conditions (2.4b) say that, at the outlet far downstream ($x = +\infty$), the water is saturated with solute, the porous medium is in its original state with porosity $\varphi_0(x, y, t)$, and the horizontal pressure gradient is to be determined as part of the problem. We take zero-flux boundary conditions on the transverse boundaries of the aquifer.

In most geological examples of interest, the (transverse) size of the reaction zone is several orders of magnitude greater than its thickness, and the details inside this zone are not of interest per se except in the way in which the cumulative effect governs the evolution of the reaction zone on this larger scale. To this end, we scale the above equations in terms of the parameter [1]

$$\varepsilon = c_{\text{eq}}/\rho \tag{2.5}$$

(typical values of ε range from 10^{-3} to 10^{-10}) and examine the limit $\varepsilon \to 0$ (the so-called large solid density limit) in the Appendix and § 2.2. We expect the thickness of the resulting reaction front separating the two values of φ to be very thin (indeed, it is $O(\varepsilon^{1/2})$), and the front itself to move very slowly. Thus, we introduce a slow dimensionless time $\tilde{t}$ by

$$\tilde{t} = \varepsilon(k c_{\text{eq}}) t, \tag{2.6}$$

and space variables $\underline{r} = (x, y)$ by

$$\underline{\tilde{r}} = (k c_{\text{eq}})^{1/2} \underline{r}, \tag{2.7}$$

along with the scaled concentration

$$\gamma = c / c_{\text{eq}}. \tag{2.8}$$

Equations (2.1)–(2.4) can then be written as (dropping the tildes and writing $d(\varphi) = \varphi D(\varphi)$, $\lambda(\varphi) = \varphi \kappa(\varphi)$)

$$\varepsilon(\varphi\gamma)_t = \nabla \cdot [d \nabla \gamma + \lambda \gamma \nabla p] + \varphi_t, \tag{2.9}$$

$$\varepsilon \varphi_t = -(\varphi_f - \varphi)^{2/3}(\gamma - 1), \tag{2.10}$$

$$\varepsilon \varphi_t = \nabla \cdot [\lambda \nabla p], \tag{2.11}$$

$$\gamma \to 0, \quad \varphi \to \varphi_f, \quad p_x \to p'_f \qquad \text{as } x \to -\infty, \tag{2.12a}$$

$$\gamma \to 1, \quad \varphi \to \varphi_0, \quad p_x \to ? \qquad \text{as } x \to +\infty. \tag{2.12b}$$

The layering of rock on a wide range of length scales can either be due to sedimentary deposition [8] or due to symmetry breaking that can occur through nucleation feedback, mechano-chemical coupling, and other processes [9]-[11]. Sedimentary layering can be be as fine as a few grain diameters (i.e., close to the lower bound of the validity of continuum theory) and can be as large as tens of meters or, in a few cases, a few hundred meters. Specific examples of sites at which layering occurs include the Simpson group sandstones [12], the marl/limestone alterations [13], and selected shales in the Woodford formation [11], all of which occur in the Anadarko basin and the St. Peter sandstone in the Michigan basin [14]. In these locations, the layering is found on the mm to m scales.

Reaction fronts in layered rock occur both naturally [15] and in the mineral extraction process. Variations in temperature or large variations in grain rate coefficients due to factors such as the presence of kinetic inhibitors in the pore fluid can result in reaction fronts that also vary from the grain scale to the scale of hundreds of meters. Therefore, geochemistry is very rich in the range of important asymptotic limits that can occur. Indeed, the ratio of the typical layer thickness to the front width can have asymptotic limits ∞, 1, and 0, all of which are relevant.

In this paper, we assume that the layering of the porous medium is the same as the thickness of the front. A specific example in which a reaction front propagates in one of the above layered rock sites and has the same thickness is taken from petroleum engineering [12]. An HCl/HF acid injection process is used to repair well damage to banded reservoirs in which the layer spacing is on the 10 mm scale. As a result of the acid injection, mineral dissolution fronts leave the bore-hole-rock contact and enter the multimineral system. Depending on the fluid injection velocities and the mineral rate coefficients, reaction front widths range from 1-100 mm. This example provides evidence of the practical relevance for the asymptotic limit considered in this paper. The details of taking the resulting distinguished limit $\varepsilon \to 0$ to obtain an effective free boundary problem are sketched in the Appendix. The resulting free boundary problem is summarized in § 2.2.

2.2. The free boundary problem. In the large solid density limit $(c_{\text{eq}}/\rho \to 0)$, we arrive at the following free boundary problem using delicate matched asymptotic/homogenization methods, which are outlined in detail in the Appendix. Upstream from the reaction front $S(x, y, t) = 0$, we have

$$\left.\begin{aligned} d_f\gamma_{xx} + D_f\gamma_{yy} + \lambda_f\gamma_x p_x + \Lambda_f\gamma_y p_y &= 0, \quad (2.13)\\ \lambda_f p_{xx} + \Lambda_f p_{yy} &= 0 \quad (2.14) \end{aligned}\right\} \quad S(x, y, t) < 0,$$

while downstream the concentration has reached its equilibrium concentration, so that

$$\left.\begin{aligned} \gamma &\equiv 1, \quad (2.15)\\ \lambda_0 q_{xx} + \Lambda_0 q_{yy} &= 0 \quad (2.16) \end{aligned}\right\} \quad S(x, y, t) > 0.$$

At the unknown reaction interface $S(x, y, t) = 0$, we have

$$\gamma = 1, \tag{2.17}$$

$$p = q, \tag{2.18}$$

$$\begin{aligned} &(p_x T_y - p_y T_x)(\lambda_f S_x^2 + \Lambda_f S_y^2) + (p_y S_x - p_x S_y)(\lambda_f S_x T_x + \Lambda_f S_y T_y)\\ &\quad = (q_x T_y - q_y T_x)(\lambda_0 S_x^2 + \Lambda_0 S_y^2) + (q_y S_x - q_x S_y)(\lambda_0 S_x T_x + \Lambda_0 S_y T_y), \end{aligned} \tag{2.19}$$

$$(\gamma_x T_y - \gamma_y T_x)\left(\frac{d_f S_x^2 + D_f S_y^2}{S_x T_y - S_y T_x}\right) = -S_t(\langle\varphi_f\rangle - \langle\varphi_0\rangle). \tag{2.20}$$

In these equations, we are using the following notation. The scaled concentration is γ, and p and q are the pressures upstream and downstream of the front $S(x, y, t)=0$. A coordinate tangent to the front is denoted by $T(x, y, t)$. The averaged constants d_f, D_f, Λ_f, λ_0, Λ_0 obtained via homogenization in the Appendix are to be understood as follows. The "dees" (d, D) and lambdas (λ, Λ) denote appropriate averages of the functions $d(\varphi)=\varphi D(\varphi)$ and $\lambda(\varphi)=\varphi\kappa(\varphi)$, respectively. The subscripts f and 0 refer to the final (altered, upstream) region and the original (unaltered, downstream) region, respectively. The lower case indicates it is averaged in the x-direction in whatever manner the homogenization dictates, while the upper case is the same for the y-direction. As an example of this notation, consider the case in which the porous medium ahead of the front is layered horizontally, and behind the front it is homogeneous as in Fig. 2.1. Then φ_f is a constant, so that $\varphi_f D(\varphi_f)$ and $\varphi_f\kappa(\varphi_f)$ are also constant, resulting in $d_f=D_f$ and $\lambda_f=\Lambda_f$. In the downstream region, $\lambda_0=\langle\varphi_0\kappa(\varphi_0)\rangle$ and $\Lambda_0=\langle\varphi_0^{-1}\kappa(\varphi_0)^{-1}\rangle^{-1}$, where the braces $\langle\,\rangle$ denote averaging over one period. In this example, homogenization dictates that, in the x-direction, the usual, arithmetic average is to be used, while, in the y-direction, the harmonic average is appropriate.

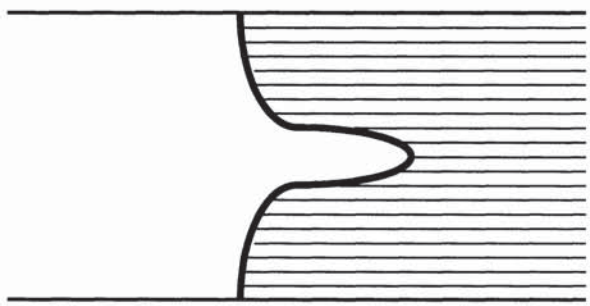

FIG. 2.1. *A porous medium that is horizontally layered ahead of the front and homogeneous behind the front.*

These equations are to be solved for γ in the upstream region (since $\gamma\equiv 1$ in the downstream region), p, q, and S subject to the asymptotic conditions

$$\gamma=0, \quad \varphi=\varphi_f, \quad p_x=p_f' \qquad \text{as } x\to-\infty \tag{2.21}$$

and

$$\varphi=\varphi_0 \qquad \text{as } x\to+\infty. \tag{2.22}$$

Note that, as $x\to+\infty$, $\gamma=1$ automatically, and q_x is to be determined as part of the solution in terms of the desiderata of the problem, especially the inlet pressure gradient p_f'. On the transverse boundaries of the aquifer, which by scaling we can take as $y=0$, π, we impose the no-flow boundary conditions γ_y, p_y, $q_y=0$.

3. Linearized shape stability analysis. We now follow the method used in references [1], [2] in which we studied the shape stability of the reaction interface $S(x, y, t)=0$ when the porous medium was homogeneous. In particular, we explicitly compute the planar solutions and thus use a linearized stability analysis to examine the stability of perturbations of the form *cosmy*, which, for $m=0, 1, \ldots$, form a complete set. We obtain a formula for the spectrum of the linearized problem for each m and compare it with that derived for the homogeneous case [1], [2] to determine if the layering has a stabilizing or destabilizing effect.

3.1. Planar solutions. We seek planar solutions for which the front moves in the x-direction with constant velocity V to be determined; that is,

$$S(x, y, t) = x - Vt, \tag{3.1}$$

and hence the perpendicular coordinate is given by

$$T(x, y, t) = y. \tag{3.2}$$

Letting all the unknown functions be of the form

$$\gamma(x, y, t) = \gamma(x - Vt), \quad p(x, y, t) = p(x - Vt), \quad q(x, y, t) = q(x - Vt)$$

expresses the fact that we seek travelling wave solutions. The planar version of equations (2.13)-(2.20) is

$$\left.\begin{aligned} &d_f\gamma'' + \lambda_f\gamma' p' = 0, && (3.3)\\ &p'' = 0 && (3.4)\end{aligned}\right\} \quad x < Vt,$$

while downstream

$$\left.\begin{aligned} &\gamma \equiv 1, && (3.5)\\ &q'' = 0 && (3.6)\end{aligned}\right\} \quad x > Vt.$$

At the unknown planar interface $x = Vt$,

$$\left.\begin{aligned} &\gamma = 1, && (3.7)\\ &p = q, && (3.8)\\ &\lambda_f p' = \lambda_0 q', && (3.9)\\ &d_f\gamma' = V(\langle\varphi_f\rangle - \langle\varphi_0\rangle). && (3.10)\end{aligned}\right\} \quad x = Vt.$$

Solving these with the asymptotic conditions

$$\gamma \to 0, \qquad p' \to p_f' \quad \text{as } x \to -\infty \tag{3.11}$$

with q' to be determined as $x \to +\infty$, we obtain (beginning with (3.4), substituting into (3.3), and so forth), using an overbar for this planar solution,

$$\bar{\gamma}(x - Vt) = e^{\alpha(x - Vt)}, \qquad \alpha = \frac{-p_f'\lambda_f}{d_f} > 0, \quad x < Vt, \tag{3.12}$$

$$\bar{p}(x - Vt) = p_f'(x - Vt), \tag{3.13}$$

$$\bar{q}(x - Vt) = \frac{p_f'}{\Gamma}(x - Vt), \qquad \Gamma = \lambda_0/\lambda_f, \tag{3.14}$$

with the velocity of the travelling front, obtained from (3.10), being

$$V = -p_f'\lambda_f/(\langle\varphi_f\rangle - \langle\varphi_0\rangle) = \frac{v_f}{\langle\varphi_f\rangle - \langle\varphi_0\rangle}, \tag{3.15}$$

where the inlet velocity $v_f = -p_f'\lambda_f$ by Darcy's law. It is not difficult to see that (3.12)-(3.15) is the unique planar solution of (2.13)-(2.20), (3.1), (3.2), and (3.11) of the form $\gamma = \gamma(x, t)$, $p = p(x, t)$, and $q = q(x, t)$, i.e., with γ, p, q simply independent of y. We now investigate the stability of these planar solutions with respect to a complete set of shape perturbations.

3.2. Linear instabilities. Let us consider small perturbations of planar fronts. Suppose that $\Delta r(y, t)$ is a small perturbation, i.e.,

$$S(x, y, t) = x - Vt + \Delta r(y, t), \tag{3.16}$$

where Δ is the size of a morphological disturbance and is much larger than the δ appearing in the Appendix. The orthogonality condition to leading order is (see (A.7))

$$S_{0,x}T_{0,x}+(S_{0,y}+S_{1,\eta})(T_{0,y}+T_{1,\eta})=0.$$

Averaging over η, we have

$$S_{0,x}T_{0,x}+S_{0,y}T_{0,y}+\langle S_{1,\eta}T_{1,\eta}\rangle=0.$$

As $\Delta\downarrow 0$, we get back the planar solution, so that $S_{1,\eta}\to 0$, $T_{1,\eta}\to 0$. Thus, $S_{1,\eta}=O(\Delta)$, $T_{1,\eta}=O(\Delta)$. Therefore, up to $O(\Delta)$, we have $S_{0,x}T_{0,x}+S_{0,y}T_{0,y}=0$. We choose T_0 as

$$T_0=y-\Delta x r_y. \tag{3.17}$$

To fix the front at $x=0$ so that the subsequent linearization is a standard procedure (albeit with more complicated equations), we change variables

$$x'=S_0(x,y,t)=x-Vt-\Delta r(y,t), \tag{3.18}$$

$$y'=T_0(x,y,t)=y-\Delta x r_y(y,t). \tag{3.19}$$

Writing the solutions of (2.13)–(2.20) as perturbations of the planar solutions (3.12)–(3.14), that is, as $\bar{\gamma}+\Delta\gamma$, $\bar{p}+\Delta p$, $\bar{q}+\Delta q$, the linearized versions of (2.13)–(2.20) in the transformed coordinates (3.18)–(3.19) are (dropping the primes)

$$\left.\begin{aligned} &d_f\gamma_{xx}+D_f\gamma_{yy}+D_f r_{yy}\bar{\gamma}'+\lambda_f(\gamma_x\bar{p}'+\bar{\gamma}'p_x)=0, && (3.20)\\ &\lambda_f p_{xx}+\Lambda_f p_{yy}+\Lambda_f r_{yy}\bar{p}'=0 && (3.21)\end{aligned}\right\}\quad x<0,$$

$$\left.\begin{aligned} &\gamma\equiv 0, && (3.22)\\ &\lambda_0 q_{xx}+\Lambda_0 q_{yy}+\Lambda_0 r_{yy}\bar{q}'=0 && (3.23)\end{aligned}\right\}\quad x>0,$$

$$\left.\begin{aligned} &\gamma=0, && (3.24)\\ &p=q, && (3.25)\\ &\lambda_f p_x=\lambda_0 q_x, && (3.26)\\ &d_f\gamma_x=r_t(-\langle\varphi_f\rangle+\langle\varphi_0\rangle) && (3.27)\end{aligned}\right\}\quad x=0.$$

These must be solved subject to the homogeneous asymptotic conditions

$$\gamma\to 0,\quad p_x\to 0\qquad \text{as } x\to-\infty, \tag{3.28}$$

$$q_x\to 0\qquad \text{as } x\to+\infty. \tag{3.29}$$

Since (3.20)–(3.29) are linear, it suffices to solve for a complete set of perturbations of the form

$$r(y,t)=e^{\sigma(m)t}\cos my, \tag{3.30a}$$

$$\gamma(x,y,t)=\gamma_m(x)\,e^{\sigma(m)t}\cos my \tag{3.30b}$$

$$p(x,y,t)=p_m(x)\,e^{\sigma(m)t}\cos my, \tag{3.30c}$$

$$q(x,y,t)=q_m(x)\,e^{\sigma(m)t}\cos my, \tag{3.30d}$$

where $\sigma(m)$ is the spectrum of the linearized problem. Substituting (3.30) into (3.20)–(3.29) gives (with primes denoting differentiation with respect to x, and dropping the sub $-\,m$ indexing wave numbers)

$$\left.\begin{aligned} &d_f\gamma''+\lambda_f p_f'\gamma'-m^2D_f\gamma-m^2D_f\alpha\,e^{\alpha x}+\lambda_f\alpha\,e^{\alpha x}p'=0, && (3.31)\\ &\lambda_f p''-m^2\Lambda_f p-m^2\Lambda_f p_f'=0 && (3.32)\end{aligned}\right\}\quad x<0,$$

$$\lambda_0 q''-m^2\Lambda_0 q-m^2\Lambda_0 p_f'/\Gamma=0,\qquad x>0, \tag{3.33}$$

$$\left.\begin{array}{ll} (3.34) & \gamma = 0, \\ (3.35) & p = q, \\ (3.36) & p' = \Gamma q', \\ (3.37) & d_f\gamma' = (-\langle\varphi_f\rangle + \langle\varphi_0\rangle)\sigma(m) \end{array}\right\} x = 0,$$

$$\gamma \to 0, \quad p' \to 0 \qquad \text{as } x \to -\infty, \tag{3.38}$$

and

$$q' \to 0 \quad \text{as } x \to +\infty. \tag{3.39}$$

Solving (3.32), (3.33) for p and q, and matching them at $x = 0$, we obtain

$$p = -p_f' + \frac{p_f'(1-(1/\Gamma))}{1+(\beta_f/\beta_0\Gamma)} e^{|m|\beta_f x}, \qquad x < 0, \tag{3.40}$$

where

$$\beta_f = \left(\frac{\Lambda_f}{\lambda_f}\right)^{1/2}, \qquad \beta_0 = \left(\frac{\Lambda_0}{\lambda_0}\right)^{1/2}, \quad \Gamma = \frac{\lambda_0}{\lambda_f}.$$

Substituting (3.40) into (3.31), we obtain

$$0 = \gamma'' - \alpha\gamma' - m^2\delta_f^2\gamma - m^2\delta_f^2\alpha\, e^{\alpha x} - \alpha^2\beta_f|m| \frac{1-\Gamma}{\Gamma+(\beta_f/\beta_0)} e^{(\alpha+\beta_f|m|)x}, \tag{3.41}$$

where

$$\delta_f = \left(\frac{D_f}{d_f}\right)^{1/2}, \qquad \alpha = -\frac{p_f'\lambda_f}{d_f} > 0.$$

Solving (3.41) for γ, we find that

$$\gamma(x) = C \exp\left(\frac{\alpha + \sqrt{\alpha^2 + 4m^2\delta_f^2}}{2} x\right) - \alpha\, e^{\alpha x} - \alpha^2\beta_f|m| \frac{1-\Gamma}{\Gamma+(\beta_f/\beta_0)}$$
$$\cdot\, e^{(\alpha+\beta_f|m|)x}(\alpha\beta_f|m| + m^2(\beta_f^2 - \delta_f^2))^{-1}.$$

By (3.34), it follows that

$$C = \alpha + \alpha^2\beta_f|m| \frac{1-\Gamma}{\Gamma+(\beta_f/\beta_0)} \cdot (\alpha\beta_f|m| + |m|^2(\beta_f^2 - \delta_f^2))^{-1}.$$

Condition (3.37) implies that

$$\gamma'|_{x=0} = \frac{\sigma(m)(-\langle\varphi_f\rangle + \langle\varphi_0\rangle)}{d_f}$$
$$= C \cdot \frac{\alpha + \sqrt{\alpha^2 + 4m^2\delta_f^2}}{2} - \alpha^2 - \alpha^2\beta_f|m|$$
$$\cdot \frac{1-\Gamma}{\Gamma+(\beta_f/\beta_0)} (\alpha + \beta_f|m|)(\alpha\beta_f|m| + m^2(\beta_f^2 - \delta_f^2))^{-1}.$$

It follows that

$$\sigma(m)=\frac{d_f}{\langle\varphi_f\rangle-\langle\varphi_0\rangle}$$

$$\tag{3.42}\begin{aligned}&\cdot\left[\alpha^2+\alpha^2\beta_f|m|\cdot\frac{1-\Gamma}{\Gamma+(\beta_f/\beta_0)}(\alpha+\beta_f|m|)(\alpha\beta_f|m|+m^2(\beta_f^2-\delta_f^2))^{-1}\right.\\&\quad+\left(-\alpha-\alpha^2\beta_f|m|\cdot\frac{1-\Gamma}{\Gamma+(\beta_f/\beta_0)}(\alpha\beta_f|m|+m^2(\beta_f^2-\beta_\delta^2))^{-1}\right)\\&\quad\left.\cdot\left(\frac{\alpha+\sqrt{\alpha^2+4m^2\delta_f^2}}{2}\right)\right].\end{aligned}$$

Let us simplify (3.42) as follows:

$$\tag{3.43}\begin{aligned}\sigma(m)&=\frac{d_f}{\langle\varphi_f\rangle-\langle\sigma_0\rangle}\left[\alpha^2+\alpha^2\beta_f\cdot\frac{1-\Gamma}{\Gamma+(\beta_f/\beta_0)}(\alpha+\beta_f|m|)\cdot\frac{1}{\alpha\beta_f+|m|(\beta_f^2-\delta_f^2)}\right.\\&\qquad+\left(\frac{\alpha+\sqrt{\alpha^2+4m^2\delta_f^2}}{2}\right)\\&\qquad\left.\cdot\left(-\alpha-\alpha^2\beta_f\cdot\frac{1-\Gamma}{\Gamma+(\beta_f/\beta_0)}\cdot\frac{1}{\alpha\beta_f+|m|(\beta_f^2-\delta_f^2)}\right)\right]\\&=\frac{d_f}{\langle\varphi_f\rangle-\langle\varphi_0\rangle}\left[\frac{\alpha^2-\alpha\sqrt{\alpha^2+4m^2\delta_f^2}}{2}+\frac{1}{2}\,\frac{1-\Gamma}{\Gamma+(\beta_f/\beta_0)}\cdot\frac{\alpha^2\beta_f}{\alpha\beta_f+|m|(\beta_f^2-\delta_f^2)}\right.\\&\qquad\left.\cdot\left((\alpha+2\beta_f|m|)-\sqrt{\alpha^2+4m^2\delta_f^2}\right)\right]\\&=\frac{d_f}{\langle\varphi_f\rangle-\langle\varphi_0\rangle}\left[\frac{\alpha^2-\alpha\sqrt{\alpha^2+4m^2\delta_f^2}}{2}+2\cdot\frac{1-\Gamma}{\Gamma+(\beta_f/\beta_0)}\cdot\frac{\alpha^2\beta_f}{\alpha\beta_f+|m|(\beta_f^2-\delta_f^2)}\right.\\&\qquad\left.\cdot\frac{\beta_f^2m^2-m^2\delta_f^2+\alpha\beta_f|m|}{(+\alpha+2\beta_f|m|)+\sqrt{\alpha^2+4m^2\delta_f^2}}\right]\\&=\frac{d_f}{\langle\varphi_f\rangle-\langle\varphi_0\rangle}\left[\frac{\alpha^2-\alpha\sqrt{\alpha^2+4m^2\delta_f^2}}{2}+2\right.\\&\qquad\left.\cdot\frac{1-\Gamma}{\Gamma+(\beta_f/\beta_0)}\cdot\frac{\alpha^2\beta_f|m|}{\alpha+2\beta_f|m|+\sqrt{\alpha^2+4m^2\delta_f^2}}\right].\end{aligned}$$

We note that

$$\sigma(m)\to-\infty\quad\text{as }|m|\to\infty,\qquad\sigma(0)=0,\quad\sigma'(0)=\frac{1-\Gamma}{\Gamma+(\beta_f/\beta_0)}\,\alpha\beta_f>0.$$

Setting $\sigma(m)=0$, we obtain

$$\tag{3.44}\begin{aligned}&\left(-\alpha+\sqrt{\alpha^2+4m^2\delta_f^2}\right)\left(\alpha+2\beta_f|m|+\sqrt{\alpha^2+4m^2\delta_f^2}\right)\\&\qquad=4\alpha|m|\beta_f\cdot\frac{1-\Gamma}{\Gamma+(\beta_f/\beta_0)},\end{aligned}$$

which yields

$$\tag{3.45}\beta_f\sqrt{\alpha^2+4m^2\delta_f^2}=-2|m|\delta_f^2+\beta_f\alpha+2\alpha\beta_f\cdot\frac{1-\Gamma}{\Gamma+(\beta_f/\beta_0)}.$$

It is easy to see that (3.45) has a unique positive solution, so that $\sigma(m)$ has the general form shown in Fig. 3.1. Set

$$\sum = \beta_f\alpha + 2\alpha\beta_f\frac{1-\Gamma}{\Gamma+(\beta_f/\beta_0)} > 0.$$

Equation (3.45) then becomes

$$\beta_f\sqrt{\alpha^2+4m^2\delta_f^2} = -2|m|\delta_f^2 + \sum.$$

Solving, we obtain

$$4(\delta_f^2-\beta_f^2)\delta_f^2 m^2 - 4\delta_f^2\sum|m| + \sum{}^2 - \beta_f^2\alpha^2 = 0$$

or

$$|m_0| = \frac{\delta_f^2\sum - \sqrt{\delta_f^4\sum^2-(\delta_f^2-\beta_f^2)\delta_f^2(\sum^2-\beta_f^2\alpha^2)}}{2(\delta_f^2-\beta_f^2)\delta_f^2}. \tag{3.46}$$

We continue to simplify (3.46) to obtain

$$|m_0| = \frac{\beta_f\alpha}{2\delta_f}\cdot\frac{\delta_f\cdot\dfrac{(\beta_f/\beta_0)+2-\Gamma}{\Gamma+(\beta_f/\beta_0)} - \left(\beta_f^2\left(\dfrac{(\beta_f/\beta_0)+2-\Gamma}{\Gamma+(\beta_f/\beta_0)}\right)^2+\delta_f^2-\beta_f^2\right)^{1/2}}{(\delta_f^2-\beta_f^2)}$$

$$= \frac{\beta_f\alpha}{2\delta_f}\cdot\frac{\left(\dfrac{(\beta_f/\beta_0)+2-\Gamma}{\Gamma+(\beta_f/\beta_0)}\right)^2-1}{\delta_f\cdot\left(\dfrac{(\beta_f/\beta_0)+2-\Gamma}{\Gamma+(\beta_f/\beta_0)}\right)+\left(\delta_f^2+\beta_f^2\left(\left(\dfrac{(\beta_f/\beta_0)+2-\Gamma}{\Gamma+(\beta_f/\beta_0)}\right)^2-1\right)\right)^{1/2}}.$$

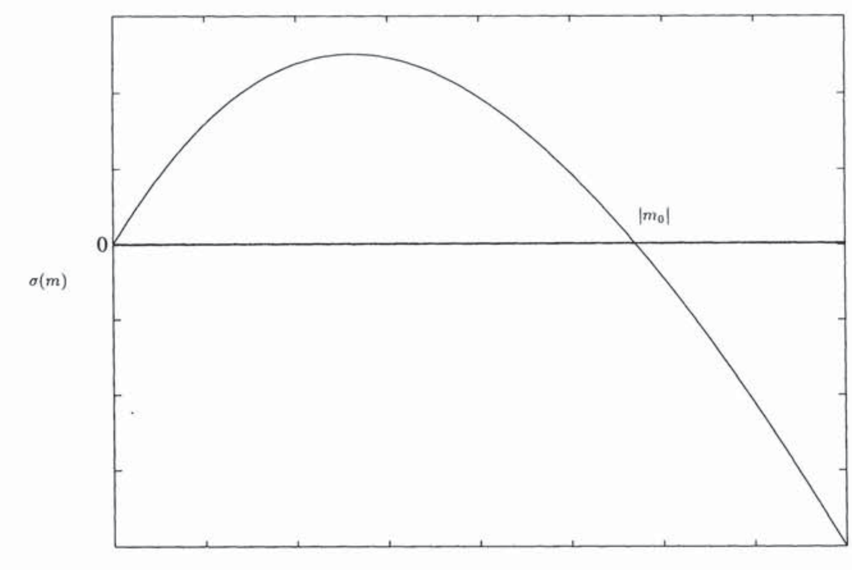

FIG 3.1. *Graph of the spectrum,* $\sigma(m)$, *of the linear problem* (3.31)–(3.39) *as a function of* $|m|$.

Let

$$s=\frac{(\beta_f/\beta_0)+2-\Gamma}{\Gamma+(\beta_f/\beta_0)}, \qquad t=\frac{\delta_f}{\beta_f};$$

then we have

$$|m_0|=\frac{\alpha}{2\delta_f}\cdot\frac{s^2-1}{ts+\sqrt{t^2+s^2-1}}. \tag{3.47}$$

Recall that

$$\alpha=-\frac{p_f'\lambda_f}{d_f}, \qquad \delta_f=\left(\frac{D_f}{d_f}\right)^{1/2},$$

so that

$$\frac{\alpha}{\delta_f}=-p_f'\cdot\frac{\lambda_f}{\sqrt{D_f d_f}}.$$

Expression (3.37) becomes

$$|m_0|=(-p_f')\frac{\lambda_f}{2\sqrt{D_f d_f}}\cdot\frac{s^2-1}{ts+\sqrt{s^2+t^2-1}}, \tag{3.48}$$

where

$$s=\frac{(\beta_f/\beta_0)+2-\Gamma}{\Gamma+(\beta_f/\beta_0)}\geqq 1, \qquad t=\frac{\delta_f}{\beta_f}>0.$$

This is the most general formula containing all of the parameters. In the case where there is layering only ahead of the front, then $t=1$, and the formula reduces to

$$\begin{aligned} |m_0|&=(-p_f')\cdot\frac{\lambda_f}{2d_f}\cdot\frac{s^2-1}{2s},\\ &=\frac{\alpha}{4}\cdot\frac{(s-1)(s+1)}{s}\\ &=\frac{\alpha}{4}\cdot\frac{(2/\beta_0)+2}{\Gamma+(1/\beta_0)}\cdot\frac{2-2\Gamma}{\Gamma+(1/\beta_0)}\cdot\frac{\Gamma+(1/\beta_0)}{(1/\beta_0)+2-\Gamma},\\ &=\alpha\cdot\frac{(\beta_0^{-1}+1)(1-\Gamma)}{(\beta_0^{-1}+\Gamma)(\beta_0^{-1}+2-\Gamma)}.\end{aligned} \tag{3.49}$$

Furthermore, if there is, in addition, no layering ahead of the front (i.e., the media is homogeneous), then $\beta_0=1$, and formula (3.49) reduces the expression in [1], [2].

3.3. Specific examples of layered porous media. In this section, we examine the effect of layering on the stability of planar fronts in two typical situations: layering only ahead of the front and layering ahead and behind the front with a fixed proportion of the medium dissolved out as the front passes. These results are compared with the case of homogeneous porous media [1], [2].

3.3.1. Layering ahead of the front. We examine the case of horizontal layering ahead of the front as depicted in Fig. 2.1. Vertical layering ahead of the front can be treated in exactly the same manner. Behind the front the porosity is a constant, which implies that $d_f = D_f =$ constant and $\lambda_f = \Lambda_f =$ constant, and hence $\delta_f = \beta_f = 1$. As mentioned earlier, a reasonable form for the permeability is $\kappa(\varphi) = K\varphi^k$, where K, $k > 0$. Thus

$$\lambda_0(\varphi) = K\varphi_0^{k+1}. \tag{3.50}$$

Since the layering is horizontal,

$$\lambda_0 = K\langle\varphi_0^{k+1}\rangle \tag{3.51}$$

and

$$\Lambda_0 = K\langle\varphi_0^{-(k+1)}\rangle^{-1}, \tag{3.52}$$

which results in

$$\beta_0^2 = \Lambda_0/\lambda_0 = \langle\varphi_0^{-(k+1)}\rangle^{-1}/\langle\varphi_0^{k+1}\rangle. \tag{3.53}$$

The important observation to make here is that, for convex functions (like x^{k+1}), the harmonic mean is less than the arithmetic mean, which results in β_0^2 being less than its value for homogeneous media, which we previously observed to be unity; i.e.,

$$\beta_0^2 < 1 = \beta_{0,h}^2. \tag{3.54}$$

Likewise, from (3.14) and (3.51),

$$\Gamma = \lambda_0/\lambda_f = \frac{K\langle\varphi_0^{k+1}\rangle}{K\varphi_f^{k+1}} = \frac{\langle\varphi_0^{k+1}\rangle}{\varphi_f^{k+1}}. \tag{3.55}$$

For a homogeneous porous medium with the same average porosity, we have

$$\Gamma_h = \langle\varphi_0\rangle^{k+1}/\varphi_f^{k+1}. \tag{3.56}$$

Again, by convexity,

$$\Gamma = \langle\varphi_0^{k+1}\rangle/\varphi_f^{k+1} > \langle\varphi_0\rangle^{k+1}/\varphi_f^{k+1} = \Gamma_h. \tag{3.57}$$

To compare the critical value m_0 with the one for a corresponding homogeneous porous medium $m_{0,h}$, we consider it, as follows, as the intersection of the branch of a hyperbola and a line (as in Fig. 3.2). In this case (using $\beta_f = \delta_f = 1$), a direct calculation from (3.42) gives, with $\alpha = -p_f'\lambda_f/d_f = \alpha_h$, that $|m_0|$ is the unique solution of

$$\begin{aligned} (\alpha^2 + 4m^2)^{1/2} &= \alpha + \frac{2|m|(1-\Gamma)}{(1/\beta_0 + 1)} \\ &< \alpha + |m|(1-\Gamma) \\ &< \alpha + |m|(1-\Gamma_h), \end{aligned} \tag{3.58}$$

the last expression with equality being the determining equation for $|m_{0,h}|$ [1], [2]. Thus, as indicated in Fig. 3.2, the horizontal layering ahead of the front stabilizes the front because the interval of unstable modes $(0, |m_0|)$ is shorter than for the corresponding homogeneous situation $(0, |m_{0,h}|)$. A physical justification for this result is relatively subtle; however, we believe that the following reasoning gives a plausible explanation. Because of the horizontal layering, (3.51) implies that the flow in the horizontal direction is dominated by those layers (which can be viewed as channels) with the highest porosity. If this effect acted alone, it would seem to promote the formation of horizontal fingers in the channels with the highest porosity. However, due to the small width of the layers, any fingers forming in these channels would be associated with high-frequency modes $m = O(\varepsilon^{-1/2})$, which are the modes that decay the most rapidly (see

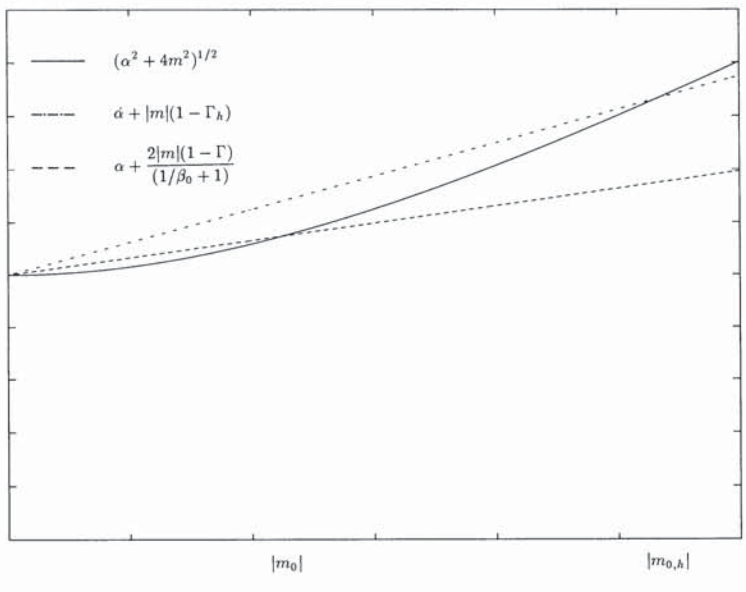

FIG 3.2. *Comparison of the critical wave number m_0 for a porous medium layered horizontally ahead of the front with a homogeneous porous medium with the same average porosity.*

Fig. 3.1). Therefore, any potentially unstable mode must be associated with a frequency that spans a number of neighboring channels. Now (3.52) implies that flow in the vertical direction is dominated by the channels with the smallest porosity (equivalently, by the harmonic mean of the permeability, which is smaller than the arithmetic mean). This serves to inhibit the formation of unstable fingers that span a number of neighboring channels. By exactly the same type of analysis, we can show that vertical layering ahead of the front has a destabilizing effect.

3.3.2. Layering ahead and behind the front. Here we consider the situation in which the reactive fluid impinges on a layered porous medium dissolving out a fixed proportion at every location and leaving behind a similarly layered medium with higher porosity as in Fig. 3.3 with

$$\varphi_0(x, y) = \theta\varphi_f(x, y), \qquad 0 < \theta < 1, \tag{3.59}$$

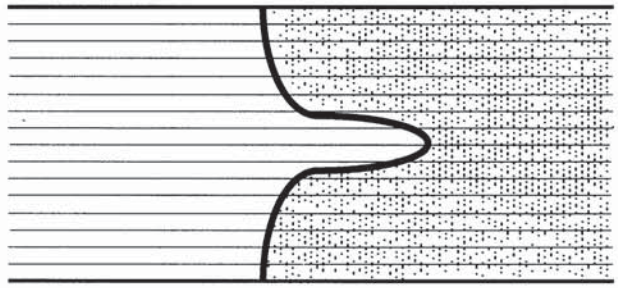

FIG. 3.3. *Reactive front moving through a horizontally layered porous medium, dissolving out a fixed proportion of the medium and leaving behind a similarly layered porous medium.*

where θ is the fixed proportion dissolved out. Again, we only treat the horizontally layered situation—the similar vertically layered case can be treated analogously.

In this case,

$$\beta_f^2 = \langle \varphi_f^{-(k+1)} \rangle^{-1} / \langle \varphi_f^{k+1} \rangle, \tag{3.60}$$

$$\beta_0^2 = \frac{\langle \varphi_0^{-(k+1)} \rangle^{-1}}{\langle \varphi_0^{k+1} \rangle} = \frac{\theta^{k+1} \langle \varphi_f^{-(k+1)} \rangle^{-1}}{\theta^{k+1} \langle \varphi_f^{k+1} \rangle} = \beta_f^2, \tag{3.61}$$

and

$$\Gamma = \lambda_0 / \lambda_f = \frac{\langle \varphi_0^{(k+1)} \rangle}{\langle \varphi_f^{k+1} \rangle} = \theta^{k+1} \frac{\langle \varphi_f^{k+1} \rangle}{\langle \varphi_f^{k+1} \rangle} = \theta^{k+1} = \Gamma_h. \tag{3.62}$$

Thus, using (3.47) and the above relations,

$$|m_0| = \frac{\alpha}{2\delta_f} \left[\frac{s^2 - 1}{ts + (s^2 + t^2 - 1)^{1/2}} \right], \tag{3.63}$$

where $s = (3 - \Gamma)/(\Gamma + 1) = s_h$, the value that enters the homogeneous medium expression, where $t = \delta_f / \beta_f$, and

$$\frac{\alpha}{\delta_f} = -p_f' \frac{\lambda_f}{d_f} \cdot \left(\frac{d_f}{D_f} \right)^{1/2} = -p_f' \frac{\lambda_f}{(d_f D_f)^{1/2}}. \tag{3.64}$$

If $t = 1 = t_h$ and $\alpha / \delta_f = \alpha_h$, then (3.63) is the expression for the homogeneous cutoff $|m_{0,h}|$. Since the right-hand side of (3.63) is a decreasing function of t, having $t < t_h = 1$ (i.e., the diffusion term δ_f is smaller than the flow term β_f) is a destabilizing effect if $\alpha / \delta_f > \alpha_h$. To see this from a more analytical viewpoint, we examine the case of small perturbations,

$$\varphi_f = \bar{\varphi}_f + \varepsilon \tilde{\varphi}_f, \tag{3.65}$$

where $\langle \tilde{\varphi}_f \rangle = 0$. Now

$$\begin{aligned} \varphi_f^{k+1}(x, y) &= \bar{\varphi}_f^{k+1} (1 + \varepsilon \chi_f(x, y))^{k+1} \\ &= \bar{\varphi}_f^{k+1} \left(1 + \varepsilon (k+1) \chi_f(x, y) + \binom{k+1}{2} k \varepsilon^2 \chi_f^2(x, y) + \cdots \right), \end{aligned} \tag{3.66}$$

where $\bar{\varphi}_f = \langle \varphi_f \rangle$ and $\chi_f = \tilde{\varphi}_f / \bar{\varphi}_f$. Noting that $\langle \chi_f \rangle = 0$, we obtain

$$\langle \varphi_f^{k+1} \rangle = \bar{\varphi}_f^{k+1} \left(1 + \frac{(k+1)k}{2} \varepsilon^2 p \right) \tag{3.67}$$

to lowest order in ε, where $p = \langle \chi_f^2 \rangle \geqq 0$. Similarly,

$$\langle \varphi_f^{-(k+1)} \rangle = \bar{\varphi}_f^{-(k+1)} \left(1 + \frac{(k+1)(k+2)}{2} \varepsilon^2 p \right). \tag{3.68}$$

Thus,

$$\lambda_f = K \bar{\varphi}_f^{k+1} \left(1 + \frac{(k+1)k}{2} \varepsilon^2 p \right) \tag{3.69}$$

and

$$\Lambda_f = K \bar{\varphi}_f^{k+1} \left(1 - \frac{(k+1)(k+2)}{2} \varepsilon^2 p \right), \tag{3.70}$$

which results in

$$\beta_f^2 = \frac{\Lambda_f}{\lambda_f} = \left(1 - \frac{(k+1)(k+2)}{2}\varepsilon^2 p\right)\left(1 + \frac{(k+1)k}{2}\varepsilon^2 p\right)^{-1} = (1-(k+1)^2\varepsilon^2 p). \tag{3.71}$$

Similarly, if we assume that the phenomenological function $\lambda(\varphi) = \varphi D(\varphi) = D\varphi^{d+1}$, we obtain

$$d_f = D\bar{\varphi}_f^{d+1}\left(1 + \frac{(d+1)d}{2}\varepsilon^2 p\right), \tag{3.72}$$

$$D_f = D\bar{\varphi}_f^{d+1}\left(1 - \frac{(d+1)(d+2)}{2}\varepsilon^2 p\right), \tag{3.73}$$

and hence

$$\delta_f^2 = D_f / d_f = (1-(d+1)^2\varepsilon^2 p). \tag{3.74}$$

From the above, we have

$$\begin{aligned} \frac{\alpha}{\delta_f} &= -p'_f \frac{\lambda_f}{(d_f D_f)^{1/2}} \\ &= -p'_f \frac{K\bar{\varphi}_f^{k+1}}{D\bar{\varphi}^{d+1}}\left(1 + \frac{(k+1)k}{2}\varepsilon^2 p\right) \\ &\quad \cdot \left(1 + \frac{(d+1)d}{2}\varepsilon^2 p\right)^{-1/2}\left(1 - \frac{(d+1)(d+2)}{2}\varepsilon^2 p\right)^{-1/2} \\ &= \alpha_h(1 + \tfrac{1}{2}((k+1)k + d + 1)\varepsilon^2 p) \\ &> \alpha_h \end{aligned} \tag{3.75}$$

and

$$\begin{aligned} \delta_f / \beta_f &= (1-(d+1)^2\varepsilon^2 p)^{1/2}(1-(k+1)^2\varepsilon^2 p)^{-1/2} \\ &= (1 + \tfrac{1}{2}((k+1)^2 - (d+1)^2)\varepsilon^2 p), \end{aligned} \tag{3.76}$$

which is smaller than the homogeneous value 1 if $d > k$, i.e., if diffusion (φ^{d+1}) is dominated by flow (φ^{k+1}). The converse is more complicated, since, by (3.75), $\alpha/\delta_f > \alpha_h$ always for this local analysis, and then there is a competition between the effects of α/β_f and δ_f/β_f. Analogous results can be obtained if the layering is vertical.

4. Conclusions. Using a free boundary problem [6] as the mathematical model for reactive flows in layered porous media, we obtain a closed form (3.48) for the spectrum of the linearized shape stability problem. This is used to compare the onset of instability for layered media with that for homogeneous media with the same average *porosity/permeability* in the following two typical situations: (i) layering ahead of the front and homogeneous behind, and (ii) layering ahead and behind the front. If the inlet flow (at $x = -\infty$) is horizontal and the layering is horizontal (i.e., $\varphi(x, y, t)$ is periodic in y), then in case (i) the front is more stable if the unaltered medium ahead of the front is layered than if it is homogeneous, and in case (ii) it is less stable if diffusion is dominated by the flow. The reverse results are true if the layering is vertical and the inlet flow remains horizontal. In all cases we use, in a crucial manner, that the harmonic mean is less than the arithmetic mean. On the other hand, the analysis is different in the two examples. Case (i) is done for a general layering, and case (ii) depends on the (physically reasonable assumption of the) layering in the altered and unaltered medium being related through a proportionality constant ($\varphi_0(x, y) = \theta\varphi_f(x, y)$) and uses a local analysis ($\varphi_f = \bar{\varphi}_f + \varepsilon\tilde{\varphi}_f$, $\varepsilon \ll 1$) for technical simplification.

Appendix. Derivation of effective equations and interface conditions. To illustrate the analysis, we consider the case of an initially horizontally layered medium, which, after interaction with the solvent, has a homogeneous distribution of porosity, i.e., $\varphi_0 = \varphi_b(y/\varepsilon^{1/2})$, where the period of the layering is the same as the width $\varepsilon^{1/2}$ of the reaction front.

Our strategy is to assume inner and outer multiple-scale perturbation expansions of the unknowns. The outer expansion involves the macroscopic variables x, y, and t, as well as the microscopic variable y/δ to represent the vertical periodicity on the length scale $\delta = \varepsilon^{1/2}$. The inner expansion involves the microscopic variables $S(x, y, t, \delta)/\delta$ and y/δ representing the normal coordinate to the unknown free boundary and medium periodicity, respectively, and the macroscopic variables $T(x, y, t, \delta)$ and t representing the tangential coordinate to the unknown free boundary and the time t, respectively. Redundancy in these representations is removed by exploiting the periodicity assumption. We then derive a consistent set of effective equations and interface conditions by matching averaged (i.e., macroscopically varying) inner variables to averaged outer variables.

A.1. Outer expansion. We expand each of the independent variables φ, γ, and p in a multiple-scale perturbation expansion of the form

$$\varphi_\delta = \tilde{\varphi}(x, y, y/\delta, t) = \tilde{\varphi}_0(x, y, y/\delta, t) + \delta\tilde{\varphi}_1(x, y, y/\delta, t) + \cdots. \tag{A.1}$$

Here we have used ($\tilde{\ }$) to distinguish an outer variable from an inner variable. However, within this section, dealing only with outer expansions, we drop this notation.

Perturbation equations order by order. Defining $\eta = y/\delta$ and substituting the expansions of the form (A.1) for φ, γ, and p of the form (A.1) into (2.9)–(2.11) we obtain

$O(\delta^{-2})>$

$$[d(\varphi_0)\gamma_{0,\eta} + \lambda(\varphi_0)\gamma_0 p_{0,\eta}]_\eta = 0, \tag{A.2a}$$

$$[\lambda(\varphi_0)p_{0,\eta}]_\eta = 0. \tag{A.2b}$$

Integrating (A.2b) with respect to η, dividing by $\lambda(\varphi_0)$, averaging over one period in η, and assuming that $\varphi_0 > 0$, it follows that the zeroth-order pressure function varies on the macroscopic scale only

$$p_0 = p_0(x, y, t). \tag{A.2c}$$

Similarly, (A.2a) implies that

$$\gamma_0 = \gamma_0(x, y, t). \tag{A.2d}$$

Exploiting the zeroth-order macroscopic dependences (A.2c) and (A.2d), the next-order equations become

$O(\delta^{-1})>$

$$[d(\varphi_0)(\gamma_{0,y} + \gamma_{1,\eta}) + \lambda(\varphi_0)\gamma_0(p_{0,y} + p_{1,\eta})]_\eta = 0, \tag{A.3a}$$

$$[\lambda(\varphi_0)(p_{0,y} + p_{1,\eta})]_\eta = 0. \tag{A.3b}$$

Applying to (A.3a) and (A.3b) a similar averaging procedure to that used for the $O(\delta^{-2})$ equations and eliminating the arbitrary functions, we obtain

$$\lambda(\varphi_0)p_{1,\eta} = p_{0,y}(\langle\lambda(\varphi_0)^{-1}\rangle^{-1} - \lambda(\varphi_0)) \tag{A.3c}$$

and

$$d(\varphi_0)\gamma_{1,\eta} = (\langle d(\varphi_0)^{-1}\rangle^{-1} - d(\varphi_0))\gamma_{0,y}. \tag{A.3d}$$

Again exploiting the fact that γ_0 and p_0 are macroscopic quantities, the next-order equations are

$O(\delta^0)>$

$$\begin{aligned}
&(d(\varphi_0)\gamma_{0,x} + \lambda(\varphi_0)\gamma_0 p_{0,x})_x \\
&+[d(\varphi_0)(\gamma_{0,y} + \gamma_{1,\eta}) + \lambda(\varphi_0)\gamma_0(p_{0,y} + p_{1,\eta})]_y \\
&+[d(\varphi_0)\gamma_{1,x} + \lambda(\varphi_0)\gamma_0 p_{1,y} + \lambda(\varphi_0)\gamma_1 p_{0,y} \\
&\quad + d'(\varphi_0)\varphi_1\gamma_{0,y} + \lambda(\varphi_0)\varphi_1\gamma_0 p_{0,y} \\
&\quad + d'(\varphi_0)\varphi_1\gamma_{1,\eta} + d(\varphi_0)\gamma_{2,\eta} \\
&\quad + (\lambda'(\varphi_1)\varphi_1\gamma_0 + \lambda(\varphi_0)\gamma_1)p_{1,\eta} \\
&\quad + \lambda(\varphi_0)\gamma_0 p_{2,\eta}]_\eta + \varphi_{0,t} = 0,
\end{aligned} \tag{A.4a}$$

$$-(\varphi_f - \varphi_0)^{2/3}(\gamma_0 - 1) = 0, \tag{A.4b}$$

$$\begin{aligned}
&(\lambda(\varphi_0)p_{0,x})_x + (\lambda(\varphi_0)p_{0,y})_y + (\lambda(\varphi_0)p_{1,\eta})_y \\
&+(\lambda'(\varphi_0)\varphi_1 p_{0,y} + \lambda(\varphi_0)p_{1,y})_\eta \\
&+(\lambda'(\varphi_0)\varphi_1 p_{1,\eta} + \lambda(\varphi_0)p_{2,\eta})_\eta = 0.
\end{aligned} \tag{A.4c}$$

Let $S_0(x, y, t) = 0$ denote the limit free boundary surface; then (A.4b) implies that $\varphi_0 = \varphi_f$ (upstream from the front, i.e., when $S_0(x, y, t) < 0$) or $\gamma_0 = 1$ (downstream from the front, i.e., when $S_0(x, y, t) > 0$).

Effective equations downstream from the front $S_0(x, y, t) > 0$. From (A.3d), we see that $\gamma_{1,\eta} = 0$, so that γ_1 is a macroscopic variable $\gamma_1 = \gamma_1(x, y, t)$. Averaging over η in (A.4c) and using (A.3c), we obtain the effective pressure equation

$$(\langle\lambda(\varphi_0)\rangle p_{0,x})_x + (\langle\lambda(\varphi_0)^{-1}\rangle^{-1} p_{0,y})_y = 0. \tag{A.5a}$$

Thus, in the limit $\delta = \varepsilon^{1/2} \to 0$, we have

$$\varphi_\delta \xrightarrow{w} \langle\varphi_b\rangle; \quad p_\delta \to p_0(x, y, t); \quad \gamma_\delta \to 1,$$

where $p_0(x, y, t)$ satisfies (A.5a) with $\varphi_0 = \varphi_b$.

Effective equations upstream from the front $S_0(x, y, t) < 0$. Averaging (A.4a) over η, using the fact that for $S_0(x, y, t) < 0$ $\varphi_f = \varphi_f(\eta)$, and using (A.3c) and (A.3d), we obtain the effective concentration equation

$$\begin{aligned}
&(\langle d(\varphi_f)\rangle\gamma_{0,x} - \langle\lambda(\varphi_f)\rangle\gamma_0 p_{0,x})_x \\
&+(\langle d(\varphi_f)^{-1}\rangle^{-1}\gamma_{0,y} + \langle\lambda(\varphi_f)^{-1}\rangle^{-1}\gamma_0 p_{0,y})_y = 0.
\end{aligned} \tag{A.5b}$$

Similarly averaging (A.4c), we obtain the same effective pressure equation (A.5a) as for the downstream case, but with $\varphi_0 = \varphi_f$. Thus, in the upstream region $S_0 < 0$, the solution in the limit $\delta = \varepsilon^{1/2} \to 0$ becomes

$$\varphi_\delta \xrightarrow{w} \langle\varphi_f\rangle; \quad p_\delta \to p_0(x, y, t); \quad \gamma_\delta \to \gamma_0(x, y, t).$$

A.2. Inner expansions. We expand each of the independent variables φ, γ, and p in interior multiple-scale perturbation expansions of the form

$$\varphi_\delta = \varphi_0(S(x, y, t, \delta)/\delta, T(x, y, t, \delta), y/\delta, t) + \delta\varphi_1(S/\delta, T, y/\delta, t) + \cdots, \tag{A.6a}$$

where we assume the following expansions for the normal and tangential coordinates:

$$\begin{aligned} S &= S(x, y, t; \delta) = S_0(x, y, t) + \delta S_1(x, y, y/\delta, t) + \cdots, \\ T &= T(x, y, t; \delta) = T_0(x, y, t) + \delta T_1(x, y, y/\delta, t) + \cdots. \end{aligned} \tag{A.6b}$$

Orthogonality condition. So that the chosen coordinate variables S and T are orthogonal, we impose the following orthogonality constraint:

$$0 = S_x T_x + S_y T_y = S_{0,x} T_{0,x} + (S_{0,y} + S_{1,\eta})(T_{0,y} + T_{1,\eta}) + O(\delta). \tag{A.7}$$

Pertrubation equations order by order. We define $\xi_1 = S/\delta$, $\xi_2 = T$, and $\eta = y/\delta$ substitute expansions (A.6) into (2.9)-(2.11), and gather terms to obtain

$O(\delta^{-2})>$

$$\begin{aligned} &S_{0,x}\partial_{\xi_1}[d(\varphi_0)S_{0,x}\gamma_{0,\xi_1} + \lambda(\varphi_0)\gamma_0 S_{0,x} p_{o,\xi 1}] \\ &\quad + (S_{0,y}\partial_{\xi_1} + \partial_\eta)[d(\varphi_0)(S_{0,y}\gamma_{0,\xi_1} + \gamma_{0,\eta}) \\ &\quad + \lambda(\varphi_0)\gamma_0(S_{0,y} p_{0,\xi_1} + p_{0,\eta})] = 0, \end{aligned} \tag{A.8a}$$

$$\begin{aligned} &S_{0,x}\partial_{\xi_1}[\lambda(\varphi_0)S_{0,x} p_{0,\xi_1}] \\ &\quad + (S_{0,y}\partial_{\xi_1} + \partial_\eta)[\lambda(\varphi_0)(S_{0,y} p_{0,\xi_1} + p_{0,\eta})] = 0. \end{aligned} \tag{A.8b}$$

The limiting values $\xi_1 \to \pm\infty$ correspond to the matching region where the inner expansions are matched to the outer expansions, i.e.,

$$\lim_{\xi_1 \to \pm\infty} p_0(\xi_1, \xi_2, \eta, t) = \tilde{p}_0(x_0, y_0, t),$$

$$\text{where } (x_0, y_0) \text{ satisfies } \begin{cases} 0 = S(x_0, y_0, t, \delta), \\ \xi_2 = T(x_0, y_0, t, \delta) \end{cases}$$

from which it follows that $\lim_{\xi_1 \to \pm\infty} p_{0,\eta} = 0$. We multiply (A.8b) by p_0, integrate over the region $(-\infty, \infty) \times T^1$, and integrate by parts to obtain

$$\int_{-\infty}^{\infty} \int_{T^1} \lambda(\varphi_0)[S_{0,x}^2 p_{0,\xi_1}^2 + (S_{0,y} p_{0,\xi_1} + p_{0,\eta})^2]\, d\xi\, d\eta = 0.$$

Now, since $\lambda(\varphi_0) > 0$, it follows that $S_{0,x} p_{0,\xi_1} = 0$ and $(S_{0,y} p_{0,\xi_1} + p_{0,\eta}) = 0$. Assuming that $|\nabla_{\xi_1\eta} S_0| \neq 0$ and considering the two cases $S_{0,x} \neq 0$ and $S_{0,y} \neq 0$ separately, it can be shown that p_0 is constant over the region $(-\infty, \infty) \times T^1$ from which it follows that $\tilde{p}_0$ is continuous across S_0, i.e., $\tilde{p}_0(0+) = \tilde{p}_0(0-)$.

Since $p_{0,\xi_1} = 0 = p_{0,\eta}$, (A.8a) is reduced to (A.8b) but with $\lambda(\varphi_0)$ replaced by $d(\varphi_0) > 0$. Therefore the above argument implies that $\gamma_{0,\xi_1} = 0 = \gamma_{0,\eta}$ and that $\tilde{\gamma}_0(0+) = \tilde{\gamma}_0(0-)$. Moreover, since $\gamma_0(+\infty, \xi_2, \eta, t) = \tilde{\gamma}_0 = 1$, it follows that $\gamma_0 = \gamma_0(\xi_2, \eta, t) \equiv 1$.

Collecting the $O(\delta^{-1})$ terms in the pressure equation (2.11), using the fact that S_0, S_1, T_0, and T_1 do not depend on ξ_1, and the orthogonality condition (A.7), we obtain

$$\begin{aligned} &[S_{0,x}^2 + (S_{0,y} + S_{1,\eta})^2](\lambda(\varphi_0) p_{1,\xi_1})_{\xi_1} + (S_{0,y} + S_{1,\eta})(\lambda(\varphi_0) p_{1,\eta})_{\xi_1} \\ &\quad + [\lambda(\varphi_0)\{(T_{0,y} + T_{1,\eta}) p_{0,\xi_2} + (S_{0,y} + S_{1,\eta}) p_{1,\xi_1} + p_{1,\eta}\}]_\eta = 0. \end{aligned} \tag{A.9a}$$

Similarly collecting $O(\delta^{-1})$ terms in the concentration equation (2.9), using $\gamma_{0,\xi_1} = 0 = \gamma_{0,\eta}$, the orthogonality condition (A.7), and the fact that $\gamma_0 = \gamma_0(\xi_2, \eta, t) \equiv 1$, we obtain

$$\begin{aligned}&[S_{0,x}^2 + (S_{0,y} + S_{1,\eta})^2](d(\varphi_0)\gamma_{1,\xi_1})_{\xi_1}\\ &\quad + (S_{0,y} + S_{1,\eta})(d(\varphi_0)\gamma_{1,\eta})_{\xi_1} + S_{0,t}\varphi_{0,\xi_1}\\ &\quad + [d(\varphi_0)\{(S_{0,y} + S_{1,\eta})\gamma_{1,\xi_1} + \gamma_{1,\eta}\}]_\eta = 0.\end{aligned} \tag{A.9b}$$

A.3. Asymptotic matching. Having derived equations governing the outer and inner expansions, we now present the procedure for matching the inner and outer solutions across the interface. This procedure results in jump conditions for the normal derivatives of $\tilde{\gamma}_0$ and $\tilde{p}_0$ and the eikonal equation for $S_0(x, y, t)$.

Local inversion of the transformation: $(\xi_1, \xi_2) \to (x, y)$. For matching we must express the outer variables (x, y) in terms of the inner variables (ξ_1, ξ_2). In (A.6b) we must match (ξ_1, ξ_2) to (x, y) while keeping η fixed. To achieve this, consider the nominal point (x_0, y_0) defined to be the solution of the system

$$0 = S(x_0, y_0, t; \delta), \qquad \xi_2 = T(x_0, y_0, t; \delta). \tag{A.10}$$

The solution to (A.10) yields the parametric representation $x_0 = x_0(\xi_2)$, $y_0 = y_0(\xi_2)$. We now linearize the transformations (A.10) about (x_0, y_0) and invert. Let

$$x = x_0 + \delta x_1 + \cdots, \qquad y = y_0 + \delta y_1 + \cdots, \tag{A.11}$$

substitute these into (A.6b), and expand. The $O(\delta)$ terms yield a linear system having the following solution:

$$x_1 = T_{0,y}\xi_1/J; \qquad y_1 = -T_{0,x}\xi_1/J, \tag{A.12}$$

where $J(x_0, y_0, t) = S_{0,x}T_{0,y} - S_{0,y}T_{0,x}$ is assumed to be nonzero.

Matching inner and outer expansions for γ: Combining the properties of $\tilde{\gamma}_0$ and γ_0 established in §§ A.1 and A.2, respectively, we obtain the following expansions:

Outer expansion:

$$S_0 > 0\colon\ \tilde{\gamma} = 1, \qquad S_0 < 0\colon\ \tilde{\gamma} = \tilde{\gamma}_0(x, y, t) + \delta\tilde{\gamma}_1(x, y, \eta, t) + \cdots. \tag{A.13a}$$

Inner expansion:

$$\gamma = 1 + \delta\gamma_1(\xi_1, \xi_2, \eta, t) + \cdots \tag{A.13b}$$

matching in the region $S_0 > 0$ is straightforward. To match in the region $S_0 < 0$, we substitute the expansions (A.11) for x and y into (A.13) and expand and eliminate x_1 and y_1 using (A.12) to obtain

$$\begin{aligned}\tilde{\gamma} = \tilde{\gamma}_0(x_0, y_0, t) + \delta[\tilde{\gamma}_{0,x}(x_0, y_0, t)T_{0,y}\xi_1/J - \tilde{\gamma}_{0,y}(x_0, y_0, t)T_{0,x}\xi_1/J\\ + \tilde{\gamma}_1(x_0, y_0, \eta, t)] + O(\delta^2).\end{aligned} \tag{A.13c}$$

Since $x_0 = x_0(\xi_2)$ and $y_0 = y_0(\xi_2)$, the outer expansion $\tilde{\gamma}$ has effectively been expressed in terms of the inner variables ξ_1 and ξ_2. Matching the $O(\delta)$ terms in (A.13b) and (A.13c), we obtain

$$\begin{aligned}\gamma_1(\xi_1, \xi_2, \eta, t) = \tilde{\gamma}_{0,x}(x_0, y_0, t)T_{0,y}\xi_1/J\\ - \tilde{\gamma}_{0,y}(x_0, y_0, t)T_{0,x}\xi_1/J + \tilde{\gamma}_1(x_0, y_0, \eta, t) \quad \text{as } \xi_1 \to -\infty.\end{aligned} \tag{A.13d}$$

We now use (A.9b) for γ_1 to derive jump conditions for $\tilde{\gamma}_0$. Since $x_0 = x_0(\xi_2)$ and $y_0 = y_0(\xi_2)$, it follows from (A.13d) that

$$\gamma_{1,\xi_1} = (\tilde{\gamma}_{0,x}T_{0,y} - \tilde{\gamma}_{0,y}T_{0,x})/J := F_1(\xi_2, t); \qquad \gamma_{1,\eta} = \tilde{\gamma}_{1,\eta} \quad \text{as} \quad \xi_1 \to -\infty. \tag{A.13e}$$

Since $\varphi_0 \xrightarrow{\xi_1\to-\infty} \varphi_f$ (which is independent of ξ_1), it follows that $\lim_{\xi_1\to-\infty}\varphi_{0,\xi_1}=0$. We therefore conclude that

$$\lim_{\xi_1\to-\infty}(d(\varphi_0)\gamma_{1,\xi_1})_{\xi_1}=0 \quad \text{and} \quad \lim_{\xi_1\to-\infty}(d(\varphi_0)\gamma_{1,\eta})_{\xi_1}=0.$$

Combining all these limiting conditions, we see that, in the limit $\xi_1\to-\infty$, (A.9b) becomes

$$d(\varphi_f)\{(S_{0,y}+S_{1,\eta})F_1(\xi_2,t)+\gamma_{1,\eta}\}=C \quad \text{(independent of } \eta).$$

Dividing by $d(\varphi_f)$, averaging over η, and eliminating C, we obtain

$$d(\varphi_f)(S_{0,y}+S_{1,\eta})F_1(\xi_2,t)+d(\varphi_f)\tilde{\gamma}_{1,h}=\langle d(\varphi_f)^{-1}\rangle^{-1}S_{0,y}F_1(\xi_2,t). \tag{A.14}$$

From (A.3d), $\tilde{\gamma}_{1,\eta}$ is a known function of η, so that (A.14) is an equation that can be used to determine the η dependence of S_1 and is known as the cell problem for S_1.

We now integrate (A.9b) over the region $(\xi_1,\eta)\in(-\infty,\infty)\times T^1$, use the fact that $\gamma_1(+\infty,\xi_2,\eta,t)=0$, (A.13e), and (A.14) to obtain the jump condition on $\tilde{\gamma}$

$$(\tilde{\gamma}_{0,x}T_{0,y}-\tilde{\gamma}_{0,y}T_x)\frac{(\langle d(\varphi_f)\rangle S_{0,x}^2+\langle d(\varphi_f)^{-1}\rangle^{-1}S_{0,y}^2)}{S_{0,x}T_{0,y}-S_{0,y}T_{0,x}} + (\langle\varphi_f\rangle-\langle\varphi_b\rangle)S_{0,t}=0. \tag{A.15}$$

Matching inner and outer expansions for p: Matching the $O(\delta^0)$ terms in the inner and outer expansions and differentiating, we obtain

$$\begin{aligned} p_{0,\xi_2}&=\frac{\partial}{\partial\xi_2}\tilde{p}_0^{\pm}(x_0(\xi_2),y_0(\xi_2),t)\\ &=(-\tilde{p}_{0,x}^{\pm}S_{0,y}+\tilde{p}_{0,y}^{\pm}S_{0,x})/J \quad \text{as} \quad \xi_1\to\pm\infty. \end{aligned} \tag{A.16a}$$

The $O(\delta)$ matching conditions for p are

$$\begin{aligned} p_1(\xi_1,\xi_2,\gamma,t)&=(\tilde{p}_{0,x}^{\pm}(x_0,y_0,t)T_{0,y}/J-\tilde{p}_{0,y}^{\pm}(x_0,y_0,t)T_{0,x}/J)\xi_1\\ &\quad+\tilde{p}_1^{\pm}(x_0,y_0,\eta,t) \quad \text{as} \quad \xi_1\to\pm\infty, \end{aligned}$$

where $\tilde{p}_k^{\pm}$ represent the outer expansions in the regions $S_0>0$ and $S_0<0$, respectively. These equations lead to the following derivative conditions:

$$\begin{aligned} p_{1,\xi_1}&=(\tilde{p}_{0,x}^{\pm}T_{0,y}-\tilde{p}_{0,y}^{\pm}T_{0,x})/J:=F_2^{\pm}(\xi_2,t),\\ p_{1,\eta}&=\tilde{p}_{1,\eta}^{\pm}(x_0,y_0,\eta,t) \quad \text{as} \quad \xi_1\to\pm\infty. \end{aligned} \tag{A.16b}$$

We now consider (A.9a) in the limit $\xi_1\to\pm\infty$, make use of the limiting conditions (A.16), and integrate with respect to η to obtain

$$(T_{0,y}+T_{1,\eta})\tilde{p}_{0,\xi_2}^{\pm}+(S_{0,y}+S_{1,n})F_2^{\pm}(\xi_2,t)+\tilde{p}_{1,\eta}^{\pm}=C^{\pm}\lambda(\varphi_0)^{-1} \quad \text{as} \quad \xi_1\to\pm\infty,$$

where $C^{\pm}$ are independent of η. Averaging over η and eliminating $C^{\pm}$, we obtain

$$\begin{aligned} &\lambda(\varphi_0)[(T_{0,y}+T_{1,\eta})\tilde{p}_{0,\xi_2}^{\pm}+(S_{0,y}+S_{1,\eta})F_2^{\pm}(\xi_2,t)+\tilde{p}_{1,\eta}^{\pm}]\\ &=\langle\lambda(\varphi_0)^{-1}\rangle^{-1}(T_{0,y}\tilde{p}_{0,\xi_2}^{\pm}+S_{0,y}F_2^{\pm}). \end{aligned} \tag{A.17}$$

We now integrate (A.9a) over the region $(\xi_1,\eta)\in(-\infty,\infty)\times T^1$ and use (A.17), the zeroth-order orthogonality condition (A.7), and (A.16a) and (A.16b) to obtain

$$\begin{aligned} &(\tilde{p}_{0,x}^{+}T_{0,y}-\tilde{p}_{0,y}^{+}T_{0,x})(\langle\lambda(\varphi_b)\rangle S_{0,x}^2+\langle\lambda(\varphi_b)^{-1}\rangle^{-1}S_{0,y}^2)\\ &\quad+(\tilde{p}_{0,y}^{+}S_{0,x}-\tilde{p}_{0,x}^{+}S_{0,y})(\langle\lambda(\varphi_b)\rangle S_{0,x}T_{0,x}+\langle\lambda(\varphi_b)^{-1}\rangle^{-1}S_{0,y}T_{0,y})\\ &=(\tilde{p}_{0,x}^{-}T_{0,y}-\tilde{p}_{0,y}^{-}T_{0,x})(\langle\lambda(\varphi_f)\rangle S_{0,x}^2+\langle\lambda(\varphi_f)^{-1}\rangle^{-1}S_{0,y}^2)\\ &\quad+(\tilde{p}_{0,y}^{-}S_{0,x}-\tilde{p}_{0,x}^{-}S_{0,y})(\langle\lambda(\varphi_f)\rangle S_{0,x}T_{0,x}+\langle\lambda(\varphi_f)^{-1}\rangle^{-1}S_{0,y}T_{0,y}), \end{aligned} \tag{A.18}$$

which is the jump condition for the pressure.

Acknowledgments. The authors thank F. Clarke and the members and staff of the CRM, Montreal, for their kind hospitality during the summer of 1990 when this work was initiated.

REFERENCES

[1] J. CHADAM, P. ORTOLEVA, AND A. SEN, *Reactive-infiltration instabilities*, IMA J. Appl. Math., 36 (1987), pp. 207-220.

[2] ———, *Weakly nonlinear stability of reaction—infiltration interfaces*, SIAM J. Appl. Math., 48 (1988), pp. 1362-1378.

[3] J. CHADAM, A. PEIRCE, AND P. ORTOLEVA, *Stability of reactive flows in porous media: Coupled porosity and viscosity changes*, SIAM J. Appl. Math., 31 (1991), pp. 684-692.

[4] J. CHADAM, J. HETTMER, E. MERINO, C. MOORE, AND P. ORTOLEVA, *Geochemical self-organization I: Feedback mechanisms and modelling approach*, Amer. J. Sci., 287 (1987), pp. 979-1007.

[5] J. CHADAM, E. MERINO, P. ORTOLEVA, AND A. SEN, *Self-organization in water-rock interaction systems II: The reactive-infiltration instability*, Amer. J. Sci., 287 (1987), pp. 1008-1040.

[6] J. XIN, A. PEIRCE, J. CHADAM, AND P. ORTOLEVA, *Reactive flows in layered porous media I: Homogenization of free boundary problems*, submitted.

[7] W. CHEN AND P. ORTOLEVA, *Reaction front fingering in carbonate—cemented sandstones*, Earth-Science Rev., 29 (1990), pp. 183-198.

[8] F. J. PETTIJOHN, *Sedimentary Rocks*, 3rd ed., Harper and Row, New York, 1975.

[9] T. DEWERS AND P. ORTOLEVA, *The role of geochemical self-organization in the migration and trapping of hydrocarbons*, Appl. Geochem., 3 (1988), pp. 287-316.

[10] ———, *A coupled reaction/transport/mechanical model for intergranular pressure solution, stylolites, and differential compaction and cementation in clean sandstones*, Geochim. Cosmochim. Acta, 54 (1990), pp. 1609-1625.

[11] P. ORTOLEVA AND Z. AL-SHAIEB, *Genesis and dynamics of basin compartments and seals*, Amer. J. Sci., 1992, to appear.

[12] V. TIGERT AND Z. AL-SHAIEB, *Pressure seals: Their diagenetic banding patterns*, in Self Organization in Geological Systems, Proc. of a Workshop held 26-30 June 1988, University of California at Santa Barbara, P. Ortoleva, B. Hallet, A. McBirney, I. Meshri, R. Reeder, and P. Williams, eds., Earth-Science Rev., 29 (1990).

[13] W. RICKEN, *Diagenetic Bedding*, Springer-Verlag, Berlin, 1986.

[14] L. D. SHEPHERD, P. A. DRZEWIECKI, J. M. BAHR, AND A. SIMO, *Silica budget for a diagenetic seal*, in Deep Basin Compartments and Seals, AAPG Memoir, 1992, submitted.

[15] H. C. GRANGER AND C. G. WARREN, Econom. Geology, 64 (1969).